Generalized Polynomial Chaos for robust modelling of Nonlinear Energy Sinks used to mitigate dynamic instabilities in braking systems

Ch. SNOUN[a], B. BERGEOT[b], S. BERGER[c]

INSA Centre Val de Loire, Université d'Orléans,
Université de Tours, LaMé EA 7494,
3 Rue de la Chocolaterie, CS 23410, 41034 Blois Cedex, France
a. cherif.snoun@insa-cvl.fr
b. baptiste.bergeot@insa-cvl.fr
c. sebastien.berger@insa-cvl.fr

Abstract:

This paper investigates the passive mitigation of a squeal noise problem in nonlinear dry friction systems with uncertain parameters by means of Nonlinear Energy Sinks (NESs). The study is based on a mechanical system which is composed of two ungrounded NESs attached to the well-known Hultèn's two degrees of freedom model. The random dispersions of the friction coefficient and the damping ratio make the system unstable. In fact, the sensitivity of these parameters is such that the steady state of the mechanical system is discontinuous and presents a jump. This jump induces areas in which the efficiency of the NESs is either high or low. Two approaches using generalized Polynomial Chaos (gPC) are developed to identify this jump and to predict the boundary values of the uncertain parameters for which the NESs can act or not. The gPC methods prove their capacities to predict the discontinuity. Thus, this analysis allows to estimate the Propensity to undergo an Harmless Steady-State Regime (PHSSR) of the oscillation by the NESs. Finally, the results are compared with the prohibitive Monte-Carlo (MC) method which is considered as the reference method. There is a good compromise between computational cost and accuracy using the gPC methods.

Keywords: Friction-induced vibration, Nonlinear Energy Sinks, Uncertainty, Robust approach, generalized Polynomial Chaos.

Contents

1 Introduction

In the working process of the braking system, squealing noise may be produced if the system comes into an unstable state. It may affect the user comfort and increases the customer complaints. Developing strategies to better understanding and control instabilities is therefore crucial.

Several researchers have been developed to understand the mechanisms generating noise and to predict it [1, 2, 3]. Friction-induced vibrations or dynamic instabilities are the scientific terms almost used. These phenomena can appear by the generation of Limit Cycle Oscillation (LCO) induced by dry friction. They are explained, in most studies of self-excited systems, by the coupling of the tangential and normal modes [4, 5, 6]. As a way to model these dynamic instabilities related to friction, the well-known two degrees of freedom Hultèn's model [7, 8] has been widely used and it is also considred as the primary system in this paper.

In order to mitigate LCO, we propose to use the concept of Targeted Energy Transfer (TET). In the last decades, TET has become an important passive control technique for reducing or eliminating unwanted vibrations [9]. It consists to attach a nonlinear device also named Nonlinear Energy Sink (NES) to the main system. The NES represents a nonlinear spring mass damper with a nonlinear stiffness, typically cubic as considered in this work. It can adapt itself to the main system that it is attached to without being tuned to a specific frequency.

NES has been widely studied theoretically and experimentally. It has been applied in several applications as for vibration mitigation [10], noise reduction [11] or seismic mitigation [12]. In recent years, particular attention has been paid for the NES design in deterministic approach [13] and also in probabilistic approach incorporating uncertainty in the parameters of the model [14]. In fact, uncertainty might have a large effect on the performance of NES. In the previous work by the authors [15], two ungrounded NESs are coupled to the well-known Hultèn's model in order to mitigate or eliminate squeaking noise in the braking system. Related to the dispersion of some uncertain parameters (here the friction coefficient), the authors classified the steady-state response regimes in two main regimes: the first is mitigated regimes which are composed by complete suppression regimes, periodic response regimes and strongly modulated responses regimes and the second is unmitigated regimes. The authors

showed that the prediction of the boundary value between strongly modulated responses and no mitigation responses is not performed. For that, it becomes necessary to take into account these uncertainties in the study of the dynamical behavior of the system.

In the literature, several probabilistic approaches are used for propagating uncertainties in a deterministic model (DM) of a mechanical system and then to evaluate the quantity of Interest (QoI) which is a response from the DM. The generalized Polynomial Chaos (gPC) method is a well-known metamodel using for quantification of uncertainties. It is a less costly alternative to the Monte Carlo (MC) approach which is often used as reference [16]. The gPC method expands the QoI of the DM in series of polynomials of uncertain variables. Many papers using the gPC method have been published as for the stability analysis of a break system [17, 18] and more recently for the stability analysis of a clutch system [19].

In this paper, the well-known Hultèn's model coupled to two ungrounded NESs is used. As explained above, a friction system coupled to NES may be in a regime with harmful LCO or not related to the dispersion of the uncertain parameters. Moreover, the transition from the mitigated regimes to the unmitigated regimes implies a jump in the steady-state amplitude profiles. Thus, the efficiency of the NES to reduce or eliminate squealing noise can switch from high to low for a slight change of the uncertain parameters. The aim of this paper is therefore to develop a method for robust modelling NES by locating this discontinuity in the dynamical behavior of the system and then to predict, with a low computational cost, the Propensity of the PHSSR. For that, two techniques using generalized Polynomial Chaos are investigated.

The article is constructed as follows: In Section 2, the gPC theory is presented. In Section 3, the two degrees-of-freedom selfexcited model coupled to NESs is introduced. In Section 4, the problem statement is formulated. In Section 5, the two jump detection methods using the gPC are developed. In Section 6, the results of the method presented in Section 5 is shown. Finally, conclusions are given in Section 7.

2 generalized Polynomial Chaos theory

2.1 generalized Polynomial Chaos

The generalized Polynomial Chaos (gPC) theory has been introduced by Wiener [20] and launched by Ghanem and Spanos [21]. The representation in the base of gPC called also Wiener-Hermite development, allows a description of the random second order function.
Consider (Ω,β,Pr) a probability space where Ω is the sample space of the random events ω, β is the σ-algebra of the subsets of Ω and Pr is the probability measure.

Let $\mu(\mu_1, ..., \mu_r)$ is a vector of r real parameters supposed to be uniformly distributed within a given interval $[a, b]^r$ and $\xi(\xi_1, ..., \xi_r)$ is a vector of r independent random variables within$[-1, 1]^r$ and obtained as

$$\mu_j(\xi_j) = \frac{a_j + b_j}{2} + \frac{b_j - a_j}{2}\xi_j, \quad (j = 1, \ldots, r). \tag{1}$$

The generalized Cameron-Martin theorem [22] determined that it is possible to express a random process $X(\xi)$ called also the Quantity of Interest (QoI) with a truncated orthogonal polynomial function series such as

$$X(\xi) \approx \sum_{j=0}^{N_p} \bar{x}_j \phi_j(\xi), \tag{2}$$

where $\bar{x}_j$ are the gPC coefficients of the stochastic process $X(\xi)$, $\phi_j(\xi)$ are orthogonal polynomial functions and $N_p = \frac{(p+r)!}{p!r!} - 1$ where p is the order of the gPC and r is the number of the uncertain parameters [23].

The polynomials ϕ_j is an orthogonal basis in the Hilbert space $L^2(\Omega, \beta, Pr)$ with the following orthogonality relation:

$$\langle \phi_i, \phi_j \rangle = \langle \phi_i, \phi_i \rangle \delta_{ij} \tag{3}$$

where δ_{ij} denotes the Kronecker delta $\delta_{ij} = \begin{cases} 0 & \text{if } i \neq j \\ 1 & \text{if } i = j \end{cases}$

and $\langle \phi_i, \phi_i \rangle = \int \phi_i \phi_i W(\xi) d\xi$ where $W(\xi)$ is the probability density function of ξ.

In this paper, the gPC coefficients are determined using a non-intrusive methods from a quite number of values of the QoI, obtained from numerical simulations of the determinstic Model (DM) presented in the Section 3. The non-intrusive method used is the regression approach which requires a minimum of $Q = kN_p$ (where k is a small integer usually equal to 2 or 3) simulations to built the coefficients. The Latin Hypercube Samples (LHS) method [24] are used to perform these Q simulations.

Using the regression approach, the coefficients are determined through the minimization of the criterion [25] given by

$$\varepsilon_{reg}^2 = \sum_{q=1}^{Q} \left[X\left(\xi^{(q)}\right) - \sum_{j=0}^{N_p} \bar{x}_j \phi_j\left(\xi^{(q)}\right) \right]^2, \tag{4}$$

where $\xi^{(q)} = \left(\xi_1^{(q)}, ..., \xi_r^{(q)}\right)$, with $q = 1, ..., Q$, is the Numerical Experimental Design (NED) chosen from the LHS method. $X\left(\xi^{(q)}\right)$ is the vector of the corresponding evaluations of the DM.

Finally, the gPC coefficients $\bar{x}_j$ are defined by

$$\bar{x} = \left(\phi^T(\xi^{(q)})\phi(\xi^{(q)})\right)^{-1} \phi^T(\xi^{(q)}) X(\xi^{(q)}), \tag{5}$$

where $\bar{x} = (\bar{x}_j, \ldots, \bar{x}_Q)$ and $\phi(\xi^{(q)})$ is the matrix defined by

$$\phi(\xi^{(q)}) = \begin{pmatrix} \phi_0(\xi^{(1)}) & \cdots & \phi_{N_p-1}(\xi^{(1)}) \\ \vdots & \ddots & \vdots \\ \phi_0(\xi^{(Q)}) & \cdots & \phi_{N_p-1}(\xi^{(Q)}) \end{pmatrix}. \tag{6}$$

2.2 Criterion for choosing the order of truncation

In this section, we present the criteria for choosing the optimal order of the truncated polynomial chaos expansion (see Eq. (2)). To obtain a good accuracy of the gPC, a high polynomial order is required

and consequently a high computational cost. It is therefore necessary to determine the optimal order of truncation in terms of accuracy and computational cost.

Let $\bar{x}_{j,p}$ and $\bar{x}_{j,p-1}$ the vectors of the gPC coefficients evaluating respectively by two successive order developments p and $p-1$. The corresponding evaluations of the QoI by the gPC are given by:

$$\begin{cases} X_p(\xi) & \approx \sum_{j=0}^{N_p} \bar{x}_j \phi_j(\xi) \\ X_{p-1}(\xi) & \approx \sum_{j=0}^{N_{p-1}} \bar{x}_j \phi_j(\xi) \end{cases} \tag{7}$$

According to the statistical characteristics of the gPC, we have:

$$\begin{cases} \hat{x}_p = \hat{x}_{p-1} = \bar{x}_0 \\ \sigma_p^2 = \frac{1}{2^r} \sum_{j=1}^{N_p} \bar{x}_j^2 \langle \phi_j^2 \rangle \\ \sigma_{p-1}^2 = \frac{1}{2^r} \sum_{j=1}^{N_{p-1}} \bar{x}_j^2 \langle \phi_j^2 \rangle \end{cases} \tag{8}$$

where $\hat{x}_p$ is the mean and σ_p^2 is the variance of the QoI by the gPC in the order p.

The error of variance $e_{\sigma^2,p}$ between two successive orders gPC is given by:

$$e_{\sigma^2,p} = \sigma_p^2 - \sigma_{p-1}^2 = \frac{1}{2^r} \sum_{j=N_{p-1}}^{N_p} \bar{x}_j^2 \langle \phi_j^2 \rangle \tag{9}$$

The mean error (in the sense of the least squares) between two successive order developments is given by:

$$\epsilon_p^2 \approx \frac{1}{N'} \sum_{k=1}^{N'} (X_p(\xi_k) - X_{p-1}(\xi_k))^2 \approx \frac{1}{N'} \sum_{k=1}^{N'} (\sum_{j=N_{p-1}+1}^{N_p} \bar{x}_j \phi_j(\xi_k))^2 \tag{10}$$

where N' is the number of samples.

From the orthogonality property of the gPC (Eq. (3)), the last error (Eq. (10)) can be written in the following form:

$$\epsilon_p^2 \approx \sum_{j=N_{p-1}+1}^{N_p} \bar{x}_j^2 \langle \phi_j^2 \rangle = e_{\sigma^2,p} \tag{11}$$

The equation (Eq. (11)) shows a very interesting result; the variance error and the mean least squares error are approximately equal between two successive order developments. It is the basic for finding a criterion for choosing the optimal order of truncation.

The criterion is based on the calculation of the decay rate of the relative error of the variance between two successive order developments and it is given by [26]:

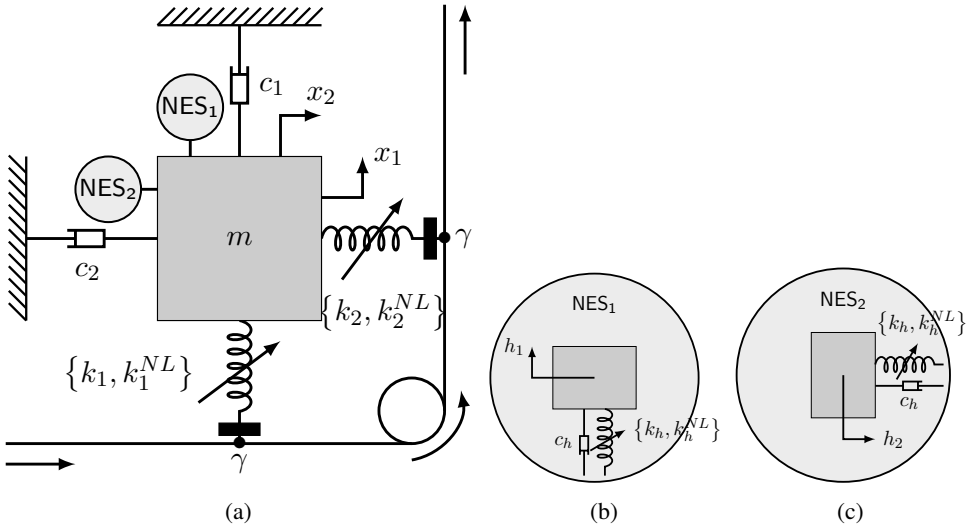

Figure 1: (a) Mechanical system with NESs. (b) Zoom on the NES_1. (c) Zoom on the NES_2.

$$\eta \ = \frac{e_{\sigma^2,p}}{\sigma_p^2} \tag{12}$$

Note that this criterion (Eq. (12)) can be estimated directly from the gPC coefficients, it is not necessary to perform additional simulations with the Deterministic Model or with the gPC to calculate these errors. This characteristic represents a major interest of the gPC method

3 Two degrees-of-freedom selfexcited model coupled to NESs

The system considered in this work is composed by the two degrees-of-freedom (DOF) Hultèn's model [7, 8], which represents the primary system, coupled to two identical NESs with masses m_h, damping coefficients c_h and cubic stiffnesses k_h^{NL}. The NESs are attached on the primary system in an ungrounded configuration as shown in Fig. 1.

The equations described the mechanical system are given by :

$$\begin{aligned}
&\frac{d^2x_1}{dt^2} + \eta_1\omega_1\frac{dx_1}{dt} + \omega_1^2 x_1 - \gamma\omega_2^2 x_2 + \varphi_1 x_1^3 - \gamma\varphi_2 x_2^3 + \\
&\quad \mu\omega_1\left(\frac{dx_1}{dt} - \frac{dh_1}{dt}\right) + \xi_h\left(x_1 - h_1\right) + \varphi_h\left(x_1 - h_1\right)^3 = 0 && \text{(13a)}\\
&\epsilon\frac{d^2h_1}{dt^2} + \mu\omega_1\left(\frac{dh_1}{dt} - \frac{dx_1}{dt}\right) + \xi_h\left(h_1 - x_1\right) + \varphi_h\left(h_1 - x_1\right)^3 = 0 && \text{(13b)}\\
&\frac{d^2x_2}{dt^2} + \eta_2\omega_2\frac{dx_2}{dt} + \omega_2^2 x_2 + \gamma\omega_1^2 x_1 + \gamma\varphi_1 x_1^3 + \varphi_2 x_2^3 + \\
&\quad \mu\omega_1\left(\frac{dx_2}{dt} - \frac{dh_2}{dt}\right) + \xi_h\left(x_2 - h_2\right)^+ \varphi_h\left(x_2 - h_2\right)^3 = 0 && \text{(13c)}\\
&\epsilon\frac{d^2h_2}{dt^2} + \mu\omega_1\left(\frac{dh_2}{dt} - \frac{dx_2}{dt}\right) + \xi_h\left(h_2 - x_2\right) + \varphi_h\left(h_2 - x_2\right)^3 = 0, && \text{(13d)}
\end{aligned}$$

where $h_1(t)$ and $h_2(t)$ (respectively $x_1(t)$ and $x_2(t)$) represent the NESs displacements (respectively the displacements of the primary system), $\eta_i = c_i/\sqrt{mk_i}$, $\omega_i = \sqrt{k_i/m}$, $\varphi_i = k_i^{NL}/m$ (with $i = 1, 2$),

$\epsilon = m_h/m$ assuming $0.01 < \epsilon < 0.1$, $\xi_h = k_h/m$, $\mu = c_h/\sqrt{mk_1}$ and $\varphi_h = k_h^{NL}/m$.

4 Problem statement

We focus our analysis on the capacity of the NESs to suppress or mitigate LCOs caused by friction-induced instabilities. An example of the direct numerical integration of the system with and without NESs is plotted in Fig. 2 which shows the displacements $x_1(t)$ as a function of the time. Four different values of the friction coefficient are used: $\gamma = 0.16$, $\gamma = 0.18$, $\gamma = 0.2$ and $\gamma = 0.22$, the other parameters are set to

$$\begin{array}{cccc} & \omega_1 = 2\pi 100, & \omega_2 = 2\pi 85, & \\ \eta_1 = 0.02, & \eta_2 = 0.06, & \varphi_1 = 10^5, & \varphi_2 = 0, \\ \epsilon = 0.05, & \xi_h = 0.001, & \mu = 0.02, & \varphi_h = 1.4 \cdot 10^5. \end{array} \tag{14}$$

Moreover, the calculation was performed on 4 seconds in order to be sure that the steady-state has been reached.

Depending on the value of the uncertain parameter, Fig. 2 schows four main types of steady-state regimes generated when two NESs is attached on the primary system: complete suppression of the instability(Fig. 2(a)), mitigation through Periodic Response (PR, Fig. 2(b)), mitigation through Strongly Modulated Response (SMR, Fig. 2(c)) or no mitigation (Fig. 2(d)). Bergeot et al. [15] have been shown these four regimes. Hereafter, mitigated regimes referred to complete suppression, PR and SMR.

We define the amplitude A_1^{wNES} of the variables x_1 of the coupled system (13) and within a steady-state regime as:

$$A_1^{wNES} = \frac{\max\left[x_1^{SSR}(t)\right] - \min\left[x_1^{SSR}(t)\right]}{2}, \tag{15}$$

where $x_1^{SSR}(t)$ is the times series of the variables x_1 obtained from the numerical integration of the coupled system (13) within the steady-state regime.

The amplitudes A_1^{wNES} and A_1^{woNES} (the amplitude of the system without NESs) are plotted as a function of the friction coefficient γ in Fig. 3 for the set of parameters.

The figure highlight a jump (or discontinuity) in the amplitude profile A_1^{wNES}. This discontinuity corresponds, when γ increases, to the transition from SMR to no suppression regime and separates mitigated regimes and unmitigated regimes.The value of γ at the jump is called mitigation limit (with respect to γ) and denoted γ_{ml}.

In the next section, we present the different methods used in this paper to detect the mitigation limit. The first method considers directly the mitigation as the QoI. The second method considers the amplitudes A_1^{wNES} as the QoI, the mitigation is deduced from it.

5 Jump detection methods

5.1 The QoI is the mitigation limit

In the first case, the mitigation limit is the quantity of interest. The method is presented in Fig. 4. It involves evaluating the mitigation limit with respect to a deterministic parameter (here we assume that β is determinist) for a given values of friction coefficicient γ.

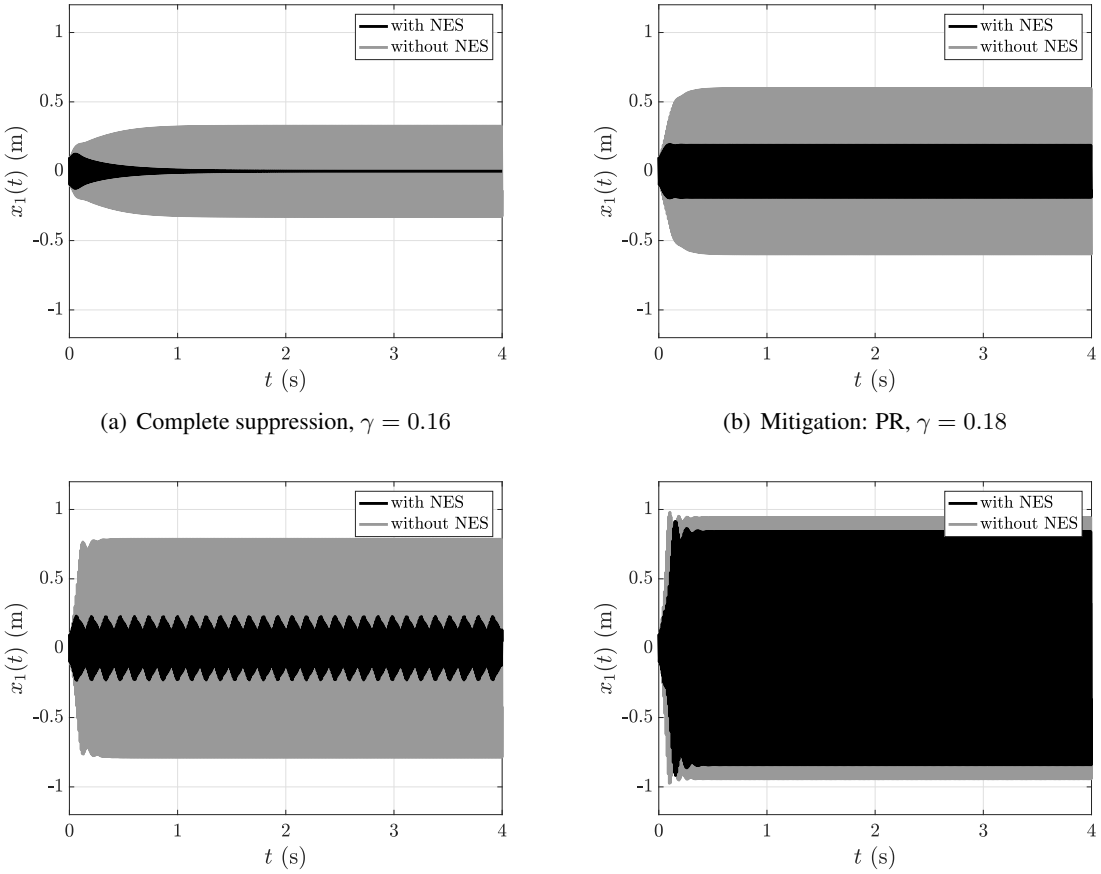

(a) Complete suppression, $\gamma = 0.16$

(b) Mitigation: PR, $\gamma = 0.18$

(c) Mitigation: SMR, $\gamma = 0.2$

(d) No suppression, $\gamma = 0.22$

Figure 2: Comparison between time serie $x_1(t)$ resulting from the numerical integration of the braking system with and without NESs. The set of parameters (14) is used.

In order to apply the gPC, the Numerical Experimental Design of the friction coefficient is built using the LHS method (see Sect.2). Then the A_1^{wNES} is calculated as a function of the deterministic damping ratio and in a given value of the uncertain friction coefficient. Fig. 5 shows two examples of the variation of A_1^{wNES} and A_1^{woNES} as a function of 250 deterministic samples of $\beta \in [1.2 \;\; 23]$ (Fig. 5(a) for $\gamma = 0.3$ and Fig. 5(b) for $\gamma = 0.4$). Then the stability analysis is performed in order to detect the bifurcation point. We denote by β_b^{woNES} the bifurcation point without NESs and β_b^{wNES} with NESs. This study allows us to delimit the stable and the unstable zones of the system. Now the gPC theory is applied, the amplitude A_1^{wNES} is evaluated only in the unstable zone when $\beta \in [1.2 \;\; \beta_b^{wNES}]$. The mitigation limit is then detected.

5.2 The QoI is the amplitude of displacement

In this section, we propose another technique to locate the discontinuity. The amplitude of displacement is now considered as the quantity of interest. Fig. 6 shows the different steps of this method. The damping ratio and the friction coefficient are considered both as uncertain parameters. The Numerical Experimental Design is then built using the LHS method (see Sect.2) with Q simulations. After the construction of the gPC coefficient, the amplitude A_1^{wNES} is evaluated using the gPC theory. Then, for a given value of β, the derivative of A_1^{wNES} is calculated (see Fig. 7). Finally, the mitigation limit is detected.

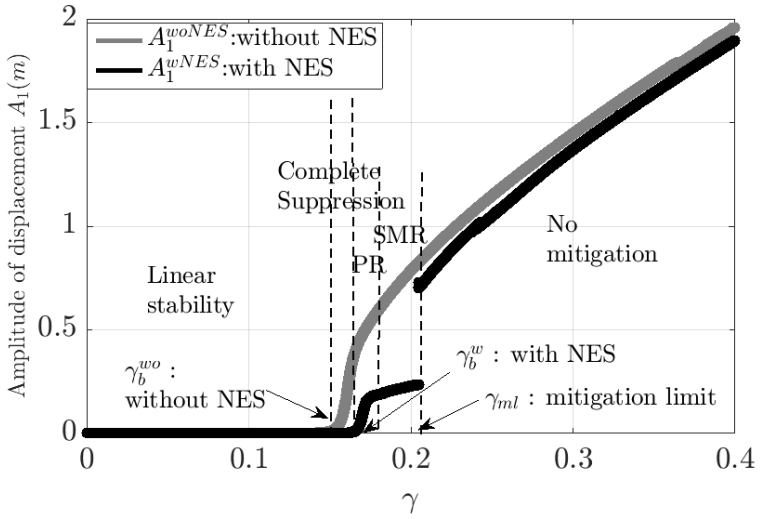

Figure 3: Amplitudes A_1^{wNES} and A_1^{woNES} as a function of the friction coefficient γ. The set of parameters (14) is used.

6 Application and results

In this section, the method presented in Sect. 5 is applied to locate the discontinuity in the steady-state amplitude profiles A_1^{wNES} (see Eq. (15) and Fig. 3) of the system under study (13).

Then the PHSSR of the oscillation by the NESs is estimated. We compute a set of S_{total} samples of the uncertain parameters within the considered uncertain space and following their distribution law. Then, the PHSSR is defined as follows

$$\text{PHSSR} = \frac{S_{\text{HSSR}}}{S_{\text{total}}} \times 100 \tag{16}$$

where S_{HSSR} is the number of samples within the region of uncertain parameters space in which the LCO of the system is mitigated or the system is stable.

6.1 Reference study

The reference is evaluated with the two algorithms (see Fig. 4 and Fig. 6). In the case that the mitigation limit is the quantity of interest, 10 000 random iterations of γ and 250 deterministic samples of β are used. The number of simulations is equal to 250 000 (250 x 10 000). In the case that A_1^{wNES} is the quantity of interest, 10 000 random iterations of the two uncertain parameters γ and β are used (see Fig. 8). The number of simulations is equal to 10 000 (100 x 100). The result of the reference is shown in Fig. 9. The value of the PHSSR is equal to 92.11% as shown in Tab. 1.

Table 1: Reference results

PHSSR(%)	Number of simulations using algorithm Fig. 4	Number of simulations using algorithm Fig. 6
92.11	250 000	10 000

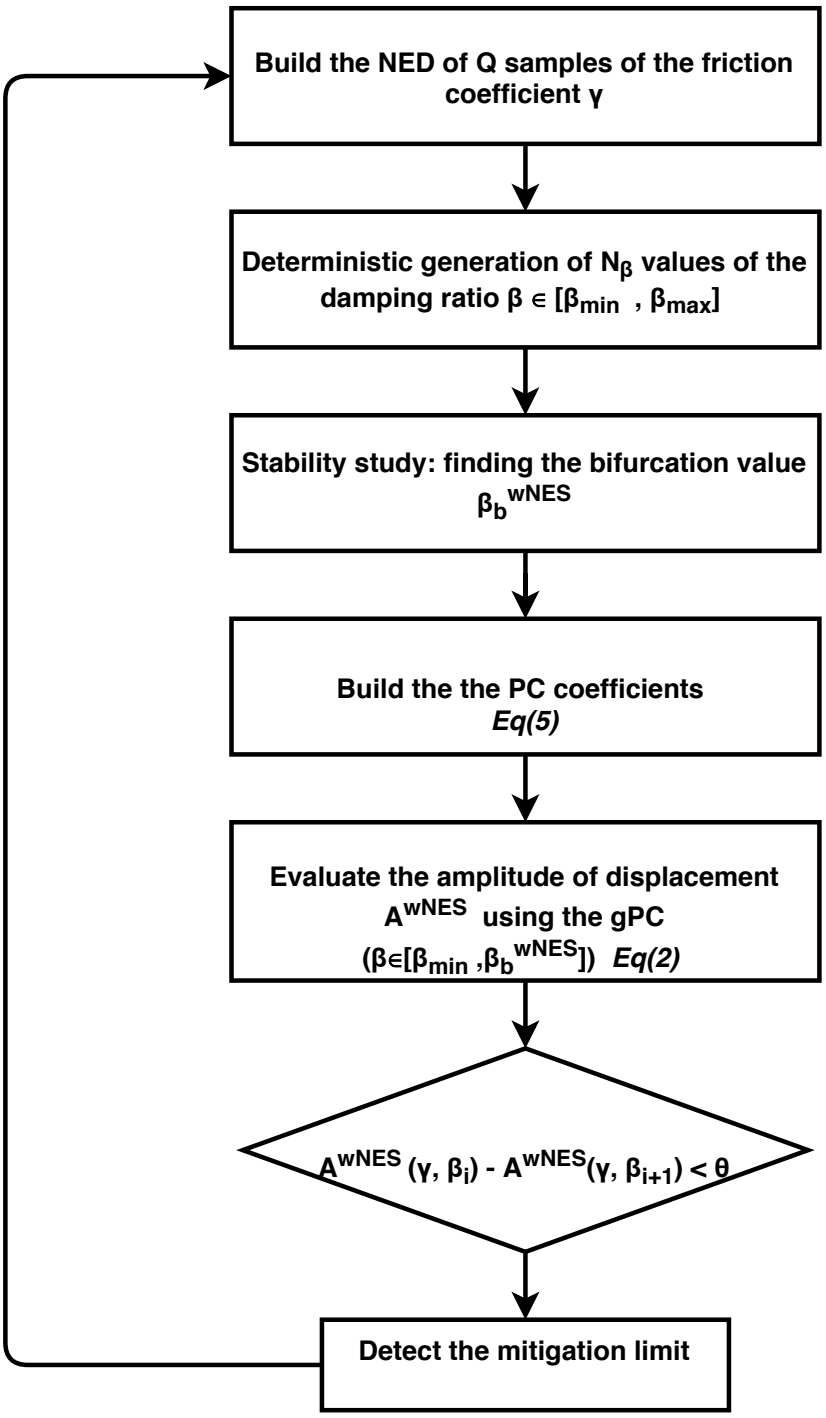

Figure 4: Algorithm applied to detect the jump when the quantity of interest is the mitigation limit.

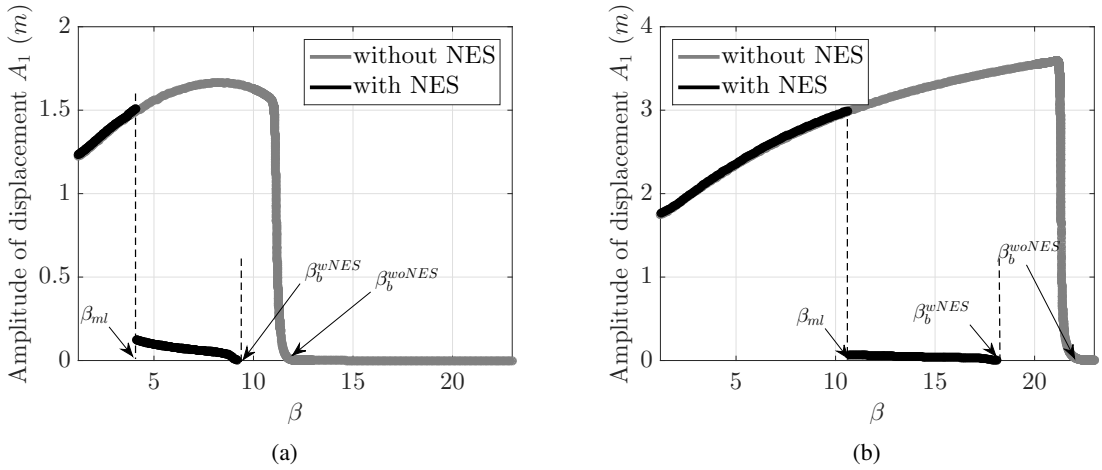

Figure 5: The amplitudes of displacement with and without NESs as a function of β: (a) $\gamma = 0.3$; (b) $\gamma = 0.4$.

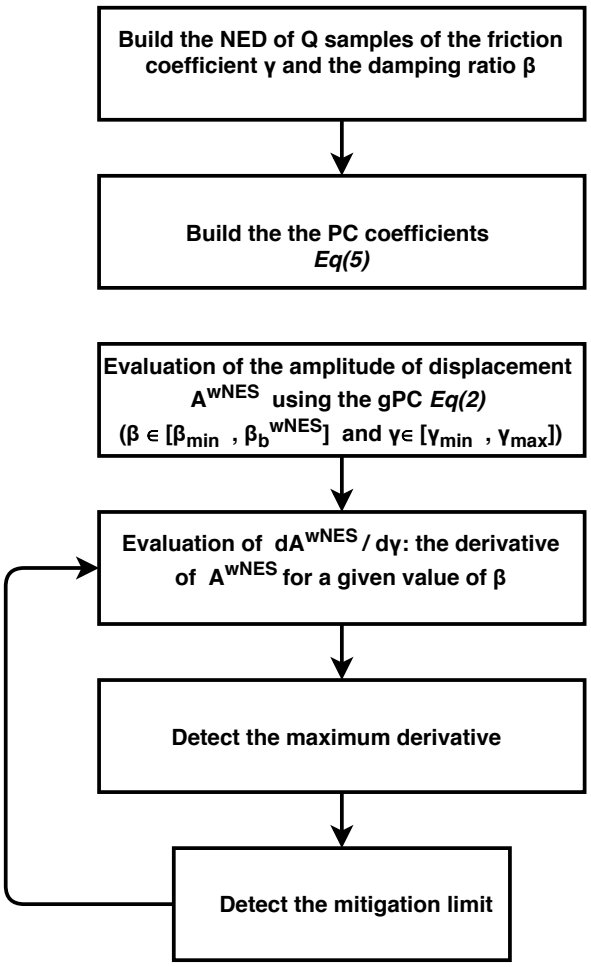

Figure 6: Algorithm applied to detect the jump in the case that the quantity of interest is the amplitude of displacement.

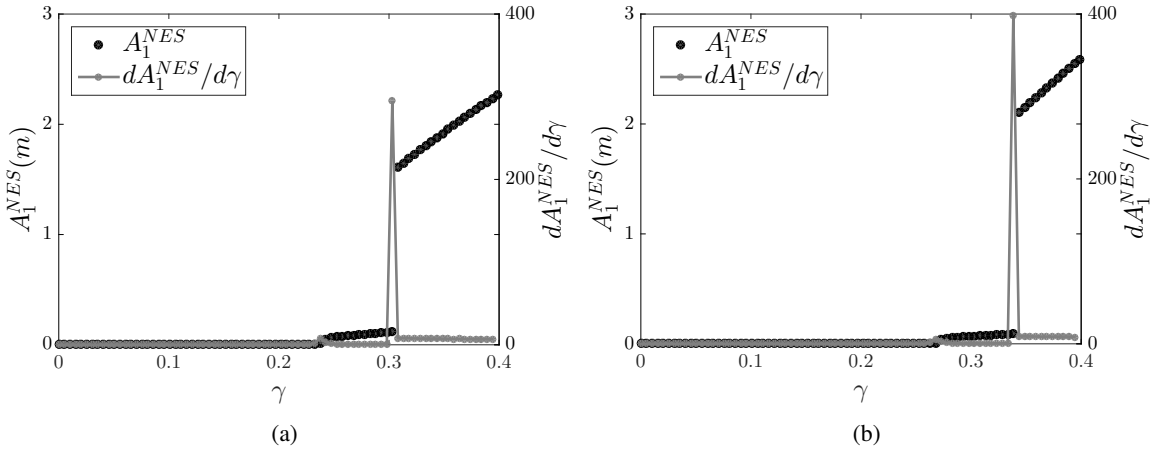

Figure 7: Example of the variation of the amplitude of displacement with NESs as a function of γ: (a) $\beta = 4.4222$; (b) $\beta = 6.7444$.

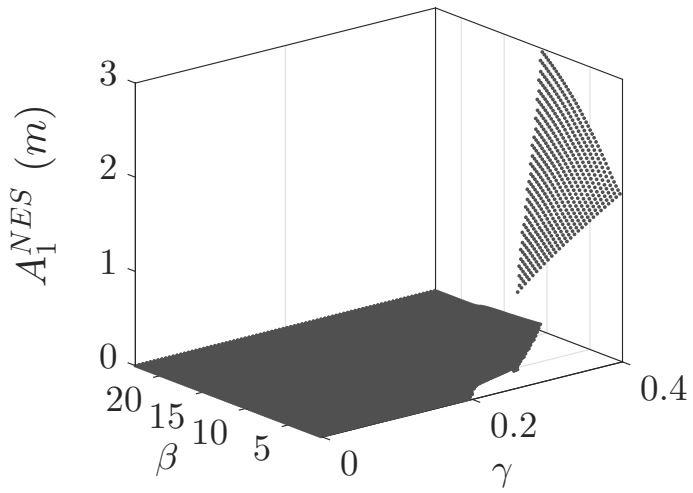

Figure 8: 10 000 deterministic simulations of the amplitude of displacement with NESs as a function of γ and β.

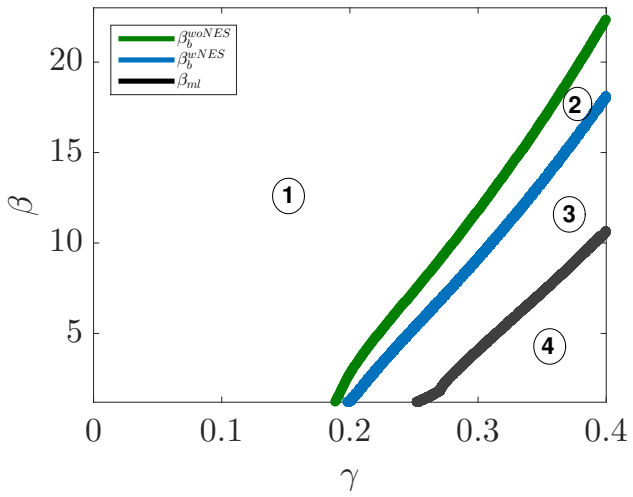

Figure 9: Evolution of the mitigation limit and Hopf bifuraction points with and without NESs using the 10 000 simulations of the reference. 1: Linear stability without NESs. 2: Linear stability with NESs. 3: Mitigation regimes (PR or SMR). 4: No mitigated regimes.

6.2 Results of the gPC approach - QoI is the mitigation limit

In this section, the algorithm presented in Fig. 4 is applied to estimate the QoI (mitigation limit) and the PHSSR.

The gPC order is changed from $p = 1$ to $p = 12$. As described in Sect. 2.1, the Latin Hypercube Samples (LHS) method is used to build the gPC coefficients using Q simulations where $Q = kN_p$ with $k = 2$.

Fig. 10 shows the results of the proposed algorithm to estimate the mitigation limit. The gPC order p is respectively equal to 2 in Fig. 10(a) and 8 in Fig. 10(b).

The different criteria illustrated in Sect. 2.2 and the comparison between the reference and the proposed method are plotted in Fig. 11. The error curves between the gPC and the reference and also between two successive chaos developments allow to verify that the criterion between two successive orders allows to choose the optimal order of truncation without knowledge of the reference. Moreover, based on the different errors plotted in Fig. 11(a), (b) and (c), $p = 6$ can be chosen as the optimal order to correctly model the quantity of interest. But for the determination of the PHSSR, the study of the error plotted in Fig. 11(d) shows that the order $p = 1$ is sufficient.

Tab. 2 shows the results for $p = 1, 2, 6, 8$ and 12. In the case where $p = 1$, the PHSSR is equal to 92% which leads to a relative error of the PHSSR compared with the reference equals to 0.119%. The mean relative error between the reference and the gPC is equal to 3.92% and the number of simulations is equal to 1000. In the case where $p = 6$, the PHSSR is equal to 92.12% which leads to a relative error of the PHSSR compared with the reference equals to 0.01%. The number of simulations increases from 1000 for $p = 1$ to 6500 for $p = 8$.

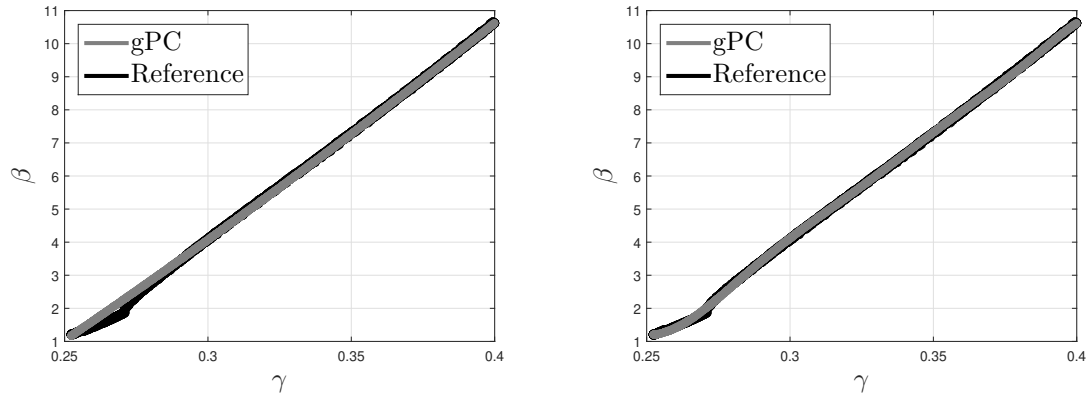

(a) (b)

Figure 10: The mitigation limit (γ_{ml},β_{ml}) : (a) $p = 2$; (b) $p = 8$.

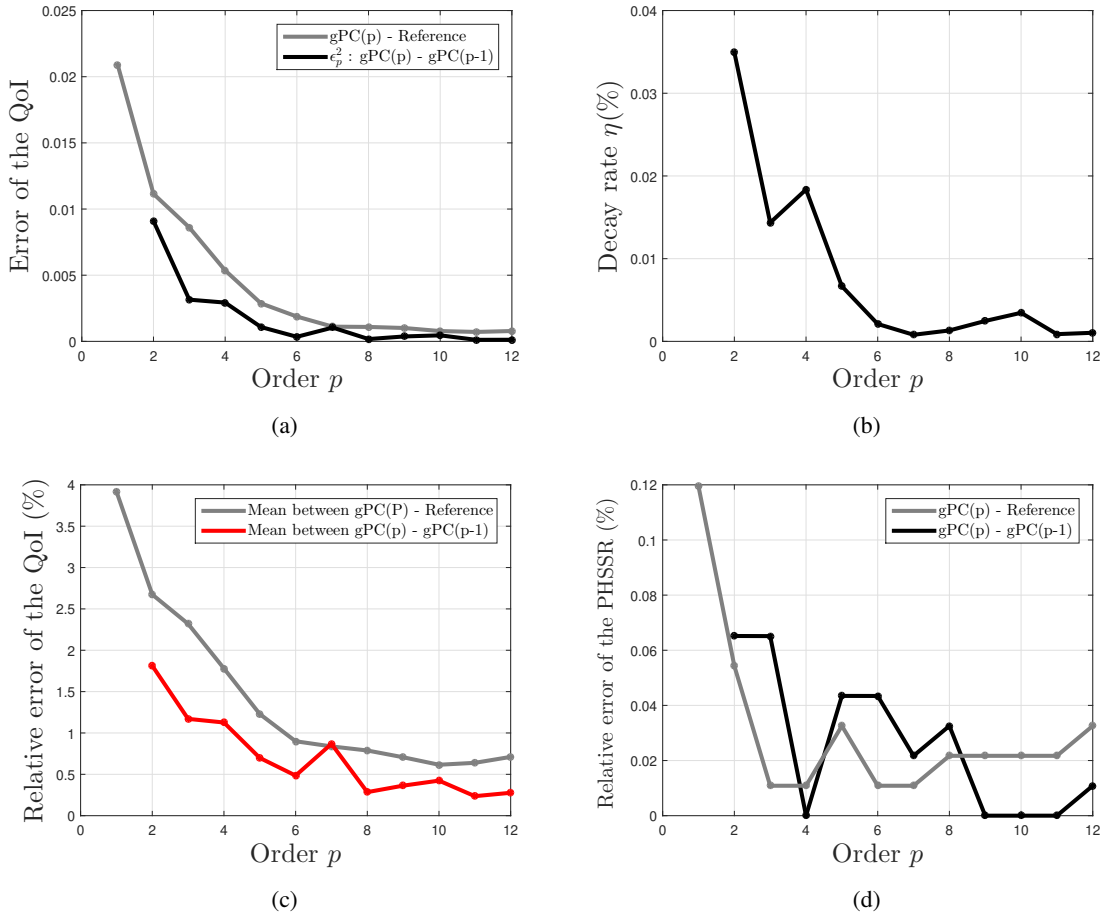

(a) (b)

(c) (d)

Figure 11: Different errors between the reference and the gPC: (a) Mean error in the sense of least squares; (b) Decay rate %; (c) Relative error of the QoI between reference and gPC; (d) Relative error of the PHSSR.

Table 2: Results using the algorithm in Fig. 4.

Order p	Number of simulations from $p=1$ to p	Mean relative error reference-gPC(%)	Decay rate(%)	PHSSR(%)	Reltive error of PHSSR reference-gPC(%)
1	1000	3.92	–	92	0.119
2	2000	2.673	0.034	92.06	0.054
6	6500	0.899	0.002	92.12	0.01
8	8750	0.788	0.0013	92.13	0.021
12	12750	0.71	0.001	92.14	0.032

6.3 Results of the gPC approach - QoI is the amplitude of displacement

In order to reduce the prohibitive cost of the first method, the algorithm presented in Fig. 6 is now applied to estimate the QoI (the A_1^{wNES}) and the PHSSR. The gPC order is changed from $p = 8$ to $p = 20$ and $Q = 3N_p$.

Fig. 12 shows the results of the proposed algorithm to estimate the mitigation limit. The gPC order p is respectively equal to 8 in Fig. 12(a) and 15 in Fig. 12(b).

The comparison between the reference and the proposed method is plotted in Fig. 13. Fig. 13(a) shows that the mean relative error of the QoI between two successive orders is not correlated with the same error between the reference and the gPC. On the other hand, Fig. 13(c) shows that the relative error of the PHSSR between two successive orders and between the reference and the gPC are correlated. Thus this last criterion and the decay rate allow to choose the optimal order of the gPC, let $p = 20$.

According to Tab. 3, the PHSSR for $p = 20$ is equal to 91.66% which leads to a relative error of the PHSSR compared with the reference equals to 0.488%. The number of simulations for the optimal order $p = 20$ represents 7 times less than the number of simulation needed by the method using the algorithm in Fig. 4 with the optimal order $p = 1$ and with a relative error of the PHSSR compared with the reference lower than 0.5%.

Table 3: Results using the algorithm in Fig. 6.

Order p	Number of simulations	Decay rate(%)	PHSSR(%)	Reltive error of PHSSR reference-gPC(%)
8	135	2.597	95.78	3.984
12	321	0.925	94.14	2.203
15	501	0.498	93.06	1.031
18	732	1.128	90.53	1.715
20	899	0.331	91.66	0.488

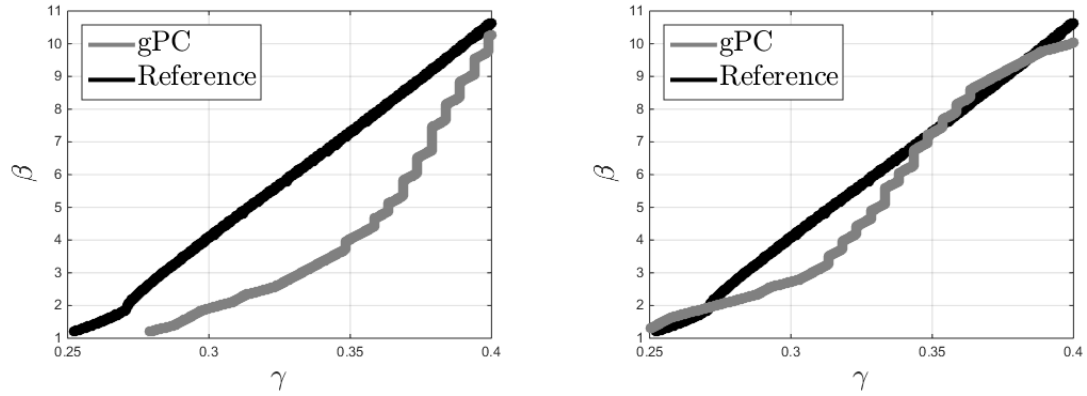

(a) (b)

Figure 12: The mitigation limit (γ_{ml},β_{ml}) : (a) $p = 8$; (b) $p = 15$.

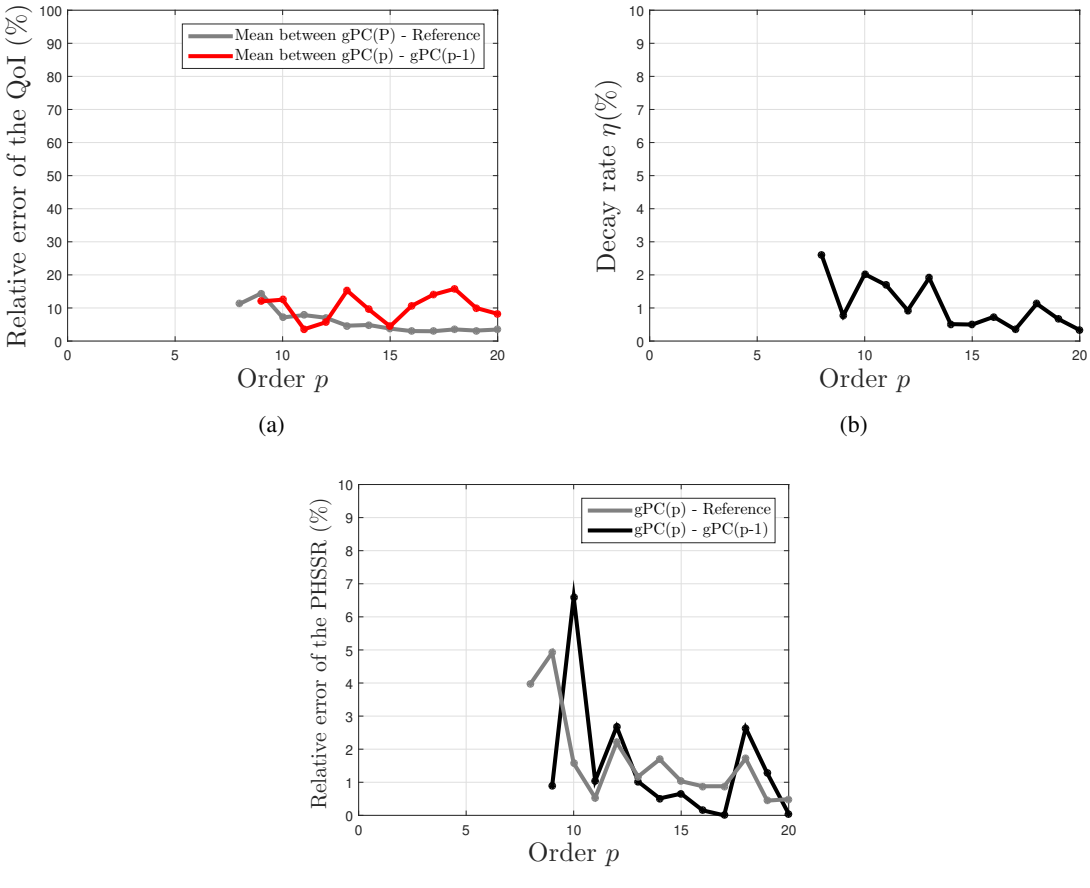

(a) (b)

(c)

Figure 13: Different errors between the reference and the gPC: (a) Relative error of the mean of the QoI; (b) Decay rate %. (c) Relative error of the PHSSR.

7 Conclusion

In this paper, a robust modelling of NES used for the brake squeal reduction is presented. For that, a simple two DOF analytical model with uncertain parameters is considered. Related to the dispersion of these uncertain parameters, the coupling of the NES with the model can generate a discontinuity in the evolution of the LCO. Two methods based on the generalized Polynomial Chaos are addressed in order to detect the jump. The first is to consider that the quantity of interest which is a response from the DM as the LCO amplitude and the second is to consider the mitigation limit is the QoI. The aim is to predict the discontinuity and not to obtain an accurate representation of the LCO amplitude. The results of these methods are noted in the following. In the case that the QoI is the LCO amplitude, a polynomial chaos expansion with an order $p = 20$ must be chosen. In the case that the QoI is the mitigation limit, a polynomial chaos expansion with an order $p = 1$ must be chosen. Note that the relative error of PHSSR between the reference and the gPC in both these two optimal configurations is less than 0.5%. However, the comparison of the number of simulations allows us to choose which technique is better in terms of computational cost and accuracy: the method that the QoI is the LCO amplitude is the most adequate.

References

[1] N.M. Kinkaid, O.M. O'Reilly, and P. Papadopoulos. Automotive disc brake squeal. *Journal of Sound and Vibration*, 267(1):105 – 166, 2003.

[2] T. Tison, A. Heussaff, F. Massa, I. Turpin, and R.F. Nunes. Improvement in the predictivity of squeal simulations: Uncertainty and robustness. *Journal of Sound and Vibration*, 333(15):3394 – 3412, 2014.

[3] D.W. Wang, J.L. Mo, M.Q. Liu, H. Ouyang, and Z.R. Zhou. Noise performance improvements and tribological consequences of a pad-on-disc system through groove-textured disc surface. *Tribology International*, 102:222 – 236, 2016.

[4] J.T. Oden and J.A.C. Martins. Models and computational methods for dynamic friction phenomena. *Computer Methods in Applied Mechanics and Engineering*, 52(1):527–634, 1985.

[5] Guillaume Fritz, Jean-Jacques Sinou, Jean-Marc Duffal, and Louis Jézéquel. Investigation of the relationship between damping and mode-coupling patterns in case of brake squeal. *Journal of Sound and Vibration*, 307(3):591–609, 2007.

[6] B. Hervé, J.-J. Sinou, H. Mahé, and L. Jézéquel. Analysis of squeal noise and mode coupling instabilities including damping and gyroscopic effects. *European Journal of Mechanics - A/Solids*, 27(2):141–160, mar 2008.

[7] J. Hultén. Friction phenomena related to drum brake squeal instabilities. In *ASME Design Engineering Technical Conferences, Sacramento, CA*, 1997.

[8] J. Hultén. Brake squeal - a self-exciting mechanism with constant friction. In *SAE Truck and Bus Meeting, Detroit, Mi, USA*, 1993.

[9] A.F. Vakakis and O.V. Gendelman. Energy pumping in nonlinear mechanical oscillators: Part II - Resonance capture. *Journal of Applied Mechanics*, 68:42–48, 2001.

[10] A. F. Vakatis, O. V. Gendelman, L. A. Bergman, D. M. McFarland, G. Kerschen, and Y. S. Lee. *Nonlinear Targeted Energy Transfer in Mechanical and Structural Systems*. Springer-Verlag, Berlin, New York, 2008.

[11] R. Bellet, B. Cochelin, P. Herzog, and P.-O. Mattei. Experimental study of targeted energy transfer from an acoustic system to a nonlinear membrane absorber. *Journal of Sound and Vibration*, 329:2768–2791, 2010.

[12] F. Nucera, A. F. Vakakis, D. M. McFarland, L. A. Bergman, and G. Kerschen. Targeted energy transfers in vibro-impact oscillators for seismic mitigation. *Nonlinear Dynamics*, 50(3):651–677, jan 2007.

[13] Tuan Anh Nguyen and Stéphane Pernot. Design criteria for optimally tuned nonlinear energy sinks—part 1: transient regime. *Nonlinear Dynamics*, 69(1-2):1–19, nov 2011.

[14] Ethan Boroson, Samy Missoum, Pierre-Olivier Mattei, and Christophe Vergez. Optimization under uncertainty of parallel nonlinear energy sinks. *Journal of Sound and Vibration*, 394:451 – 464, 2017.

[15] B Bergeot, S Berger, and S Bellizzi. Mode coupling instability mitigation in friction systems by means of nonlinear energy sinks : numerical highlighting and local stability analysis. *Journal of Vibration and Control*, 24(15):3487–3511, 2017.

[16] George S Fishman. *Monte carlo: concepts, algorithms, and applications*. Springer Series in Operations Research. Springer, New York, 1996.

[17] L. Nechak, S. Berger, and E. Aubry. Non-intrusive generalized polynomial chaos for the robust stability analysis of uncertain nonlinear dynamic friction systems. *Journal of Sound and Vibration*, 332(5):1204 – 1215, 2013.

[18] L. Nechak, S. Besset, and J.-J. Sinou. Robustness of stochastic expansions for the stability of uncertain nonlinear dynamical systems – application to brake squeal. *Mechanical Systems and Signal Processing*, 111:194 – 209, 2018.

[19] Duc Thinh Kieu, Baptiste Bergeot, Marie-Laure Gobert, and Sébastien Berger. Stability analysis of a clutch system with uncertain parameters using sparse polynomial chaos expansions. *Mechanics & Industry*, 20(1):104, 2019.

[20] Norbert Wiener. The homogeneous chaos. *American Journal of Mathematics*, 60(4):897, oct 1938.

[21] Roger G. Ghanem and Pol D. Spanos. Stochastic finite elements: A spectral approach. 1991.

[22] R.H. Cameron and W.T. Martin. The orthogonal development of non-linear functionals in series of fourier-hermite functionals. *Annals of Mathematics*, 48(2):385–392, 1947.

[23] D. Xiu and G.E. Karniadakis. The wiener–askey polynomial chaos for stochastic differential equations. *SIAM Journal on Scientific Computing*, 24(2):619–644, 2002.

[24] M.D. McKay, R.J. Beckman, and W.J. Conover. A comparison of three methods for selecting values of input variables in the analysis of output from a computer code. *Technometrics*, 21(2):239–245, 1979.

[25] M. Berveiller, B. Sudret, and M. Lemaire. Stochastic finite element: a non intrusive approach by regression. *European Journal of Computational Mechanics/Revue Européenne de Mécanique Numérique*, 15(1-3):81–92, 2006.

[26] Xiaoliang Wan and George Em Karniadakis. An adaptive multi-element generalized polynomial chaos method for stochastic differential equations. *Journal of Computational Physics*, 209(2):617 – 642, 2005.